Abstraction of atomic hydrogen by atomic deuterium from an amorphous hydrogenated silicon surface

Abstraction of atomic hydrogen by atomic deuterium from an amorphous hydrogenated silicon surface

Sumit Agarwal and Akihiro Takano[a)]
Department of Chemical Engineering, University of California, Santa Barbara, California 93106-5080

M. C. M. van de Sanden
Department of Applied Physics, Eindhoven University of Technology, PO Box 513, 5600 MB, Eindhoven, The Netherlands

Dimitrios Maroudas[b)] and Eray S. Aydil[c)]
Department of Chemical Engineering, University of California, Santa Barbara, California 93106-5080

(Received 21 May 2002; accepted 23 September 2002)

We have studied the interactions of atomic deuterium with hydrogenated amorphous silicon (a-Si:H) surfaces using surface-sensitive infrared spectroscopy. We deconvoluted the effects of the abstraction reaction from insertion and etching reactions and determined the activation energy barrier for abstraction of H by D from a-Si:H surfaces. Both abstraction and insertion are observed in our experiments conducted over times ranging from a few seconds to hundreds of seconds and sequential insertion of D eventually results in the formation of deuterated silane and etching of the film. The abstraction rate is found to be independent of temperature with an essentially zero activation energy barrier (0.011 ± 0.013 eV), consistent with an Eley–Rideal mechanism and in agreement with recent atomistic calculations. © *2002 American Institute of Physics.*
[DOI: 10.1063/1.1522400]

I. INTRODUCTION

Hydrogenated amorphous silicon (a-Si:H) and nanocrystalline silicon (nc-Si:H) films are used as the semiconductor materials in photovoltaic devices and thin-film transistors (TFTs) for flat panel displays.[1–3] Such thin Si films are commonly deposited by plasma deposition from SiH_4 containing discharges often diluted with H_2.[2] The hydrogen content of these films plays a key role in determining their electronic properties.[4] Hydrogen passivates dangling-bond defects in amorphous silicon thus increasing carrier lifetime. However, too much hydrogen incorporation leads to formation of a less dense a-Si:H network with voids and, hence, inferior electronic properties.[4] Moreover, the mobility of hydrogen in the film has been correlated with the photodegradation of a-Si:H, known as the Staebler–Wronski effect.[5]

The hydrogen concentration in a-Si:H films is determined by the surface reactions that lead to net hydrogen elimination during growth.[2,6] In order to understand the mechanism of film deposition and hydrogen incorporation, radical-surface interactions that lead to hydrogen addition and elimination must be identified and their energetics and rates must be determined. During a-Si:H deposition, numerous SiH_4 fragments generated in the plasma, including H, impinge onto the growth surface. Hence, the role of atomic hydrogen cannot be isolated from the role of other radicals, such as SiH_x $(0 \leqslant x \leqslant 3)$, which also bring hydrogen to the surface. A hydrogen atom impinging onto an a-Si:H film can abstract H from the surface, passivate a dangling bond, or insert into strained Si–Si bonds[7] (Fig. 1). Repeated sequential insertion into Si–Si bonds can lead to formation of volatile silanes and eventual etching of the film as shown schematically in Fig. 1(e). Among the various reactions that an impinging H can undergo on the a-Si:H surface, abstraction of a surface H atom may be an important pathway for H elimination from the growing film.[6,8,9]

Surface abstraction typically proceeds via two distinct mechanisms. In the first one, the Eley–Rideal (ER) mechanism, the impinging atom is not accommodated on the surface and directly abstracts another atom from the surface at the first point of its contact with the surface. In the second, more commonly observed Langmuir–Hinshelwood (LH) mechanism, both the reactants are well equilibrated with the surface and react to form the product, which subsequently desorbs.[10] Surface reactions can also proceed via an intermediate mechanism between the two extremes of ER and LH mechanisms. An example is the abstraction of a surface H atom by atomic H via a ''hot precursor'' state. In this mechanism, a ''hot'' H atom is trapped on the surface for a time period during which it can sample different sites on the surface until it finally reacts with and abstracts a bound surface hydrogen atom.[10] Although there is consensus in the literature that the abstraction of atomic hydrogen from a crystalline silicon (c-Si) surface proceeds via the ER mechanism, there is still debate about the details of the reaction and whether it proceeds directly or through a hot precursor state.[11–15] The ER and the ''hot precursor'' mechanisms are

[a)]Permanent address: Fuji Electric Corporate Research and Development, Ltd., 2-2-1, Nagasaka, Yokosuka-city 240-0194, Japan.
[b)]Current address: Department of Chemical Engineering, University of Massachusetts - Amherst, Amherst, MA 01003-3110.
[c)]Author to whom correspondence should be addressed; electronic mail: aydil@engineering.ucsb.edu

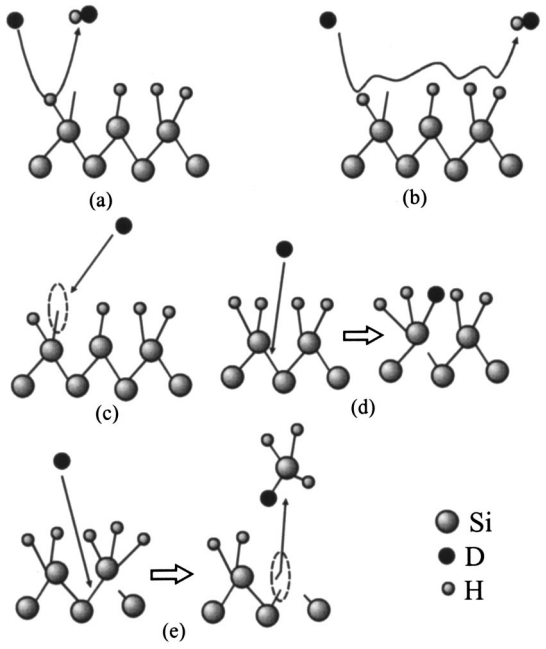

FIG. 1. Schematic illustration of the interactions of a D atom impinging onto an *a*-Si:H surface. D can abstract a surface H atom via either a direct Eley–Rideal mechanism (a) or through a hot precursor state (b), passivate a dangling bond (c), or insert into a Si–Si bond (d). Sequential insertion into Si–Si bonds leads to the formation of higher deuterated silicon hydrides and eventual etching (e).

illustrated in Figs. 1(a) and 1(b), respectively; in both cases, the reaction kinetics is expected to be first-order in the surface hydride coverage.[10] In the present work, we determined the activation energy barrier of the abstraction reaction on an *a*-Si:H surface based on first-order reaction kinetics. A low activation barrier would be consistent with both mechanisms.[10,16]

Experimental and theoretical literature on the abstraction of H(D) by atomic D(H) from *c*-Si surfaces is extensive and has been recently summarized by Dinger *et al.*[17] Briefly, Koleske *et al.*[11,13] measured an activation energy barrier of 0.022–0.043 eV for the abstraction of H by D and H on both Si(100) and Si(111) surfaces independent of the isotope. Srinivasan *et al.*[18] used *ab initio* configuration interaction (CI) theory in a collinear interaction geometry to calculate the activation energy barrier for the abstraction of hydrogen from silicon mono-hydride and silicon di-hydride in Si_4H_{10} and Si_3H_8 clusters, respectively. These authors reported a barrier of 0.239 eV for the mono-hydride and between 0.317 eV and 0.416 eV for the di-hydride configuration. Nakajima *et al.*[19] used an *ab initio* molecular-orbital method to calculate the activation energy barrier for abstraction of H from Si_nH_{2n+2} $(1 \leqslant n \leqslant 7)$ clusters. The activation energy barrier was between 0.28 and 0.46 eV, higher for smaller clusters. Using nonlocal density functional theory (DFT), Nakamura[20] calculated a zero activation energy barrier for the abstraction of hydrogen from a Si(100)-(2×1) surface modeled with a Si_9H_{14} cluster, in very close agreement with experiments.

Although there have been quantitative and mechanistic studies of H(D) abstraction reaction from *c*-Si surfaces, the reaction is more difficult to study on *a*-Si:H film surfaces. The difficulty arises from the fact that H can insert into Si–Si bonds at a comparable rate on the *a*-Si:H surface due to the presence of strained Si–Si bonds[21,22] and, hence, it is difficult to quantitatively deconvolute the effects of the two reactions on the surface H coverage. Using sensitive infrared reflection absorption spectroscopy and 20 nm thick *a*-Si:H films, von Keudell *et al.* were the first to separate the insertion and exchange reactions of H in the bulk. They showed that these reactions occurred at comparable rates at 250 °C. However, the mechanism of abstraction reaction followed by passivation, which leads to exchange of H with D (or D with H) on the surface, is different than the proposed exchange mechanism in the bulk *a*-Si:H.[23,24] Another problem in analyzing the abstraction reaction on the *a*-Si:H surface is that, though it is possible to define surface bonding sites, the disordered *a*-Si:H surface makes it difficult to quantify surface coverage. As a result, most of the studies on abstraction of H from an *a*-Si:H surface tend to be qualitative. On an *a*-Si:H surface, the abstraction reaction was first discussed by Abelson *et al.*;[8,9] these authors used mass spectrometry and isotope labeling and showed that there is an H removal mechanism from the surface with a rate that is proportional to the H flux. Muramatsu *et al.*[25] used mass spectrometry to monitor the rate of HD formation when an *a*-Si:H:D film deposited from a SiH_4/D_2 discharge was exposed to H from an H_2 plasma and calculated an activation energy barrier of 0.102 eV for abstraction. Srinivasan *et al.*[26] also used mass spectrometry to measure the appearance of gas-phase HD and SiD_4 when an *a*-Si:H film was exposed to D from a D_2 plasma at 80 Pa; they argued that the HD detected by the mass spectrometer can only be the product of an Eley–Rideal abstraction reaction occurring on the *a*-Si:H surface. However, it is not clear in their work if the abstraction reaction product, HD, is formed on the surface or in the bulk film. The authors have not considered alternative reaction pathways for the formation of HD in spite of the high chamber pressure. For example, HD can be formed from etch products like SiH_xD_{4-x} $(0 \leqslant x \leqslant 4)$ through a combination of gas-phase and surface reactions on the reactor walls. Nevertheless, Srinivasan *et al.*[26] reported energy barriers of 0.017 eV and 0.048 eV corresponding to two different plasma powers and did not discuss the unexpected dependence of the activation energy barrier on plasma power. To the best of our knowledge, the above two indirect measurements remain the only experimental measurements of the activation energy barrier for abstraction of D(H) by H(D) from an *a*-Si:H film.

In this article, we focus on determining the activation energy barrier for abstraction of H from an *a*-Si:H surface by D. Experimentally, abstraction of surface H by atomic H(D) can be monitored either by detection of the gas-phase reaction products (H_2 or HD) desorbing from the surface or by directly observing the changes in the surface H(D) coverage. The former technique is more suitable for ultra-high vacuum studies, where the reaction products can be detected without any gas-phase collisions or collisions with the chamber walls using techniques such as quadrupole or time of flight mass spectrometry. The latter approach of detecting changes on the surface is more suitable for *a*-Si:H films being deposited and post-treated by H(D) in a plasma environment. A vast

majority of the *in situ* surface diagnostics used to monitor changes in *a*-Si:H films are based on infrared (IR) detection of the different local vibrational modes of Si–H bonds. Among the different IR-based surface diagnostics, attenuated total internal reflection Fourier transform infrared (ATR-FTIR) spectroscopy[27,28] is the most suitable for a kinetic study of the abstraction reaction, because of its high sensitivity to small changes in the hydrogen concentration on the film's surface.[28–30] In our experiments, we specifically measure the changes in the H and D concentrations and bonding configurations, both on the surface and in the film using attenuated total reflection and multiple internal transmission, respectively. We also consider the possibility of simultaneous abstraction, insertion, and etching reactions that may occur on the surface and in the bulk film and isolate the effect of the surface abstraction reaction from others. Analysis of the IR spectra is based on the identification of stretching modes of the different silicon hydrides and deuterides which appear between $\sim$1950–2200 cm^{-1} and $\sim$1400–1600 cm^{-1}, respectively. Abstraction and subsequent passivation of a dangling bond by H on an *a*-Si:H surface cannot be observed using surface infrared spectroscopy as there is no net change in the concentration of Si–H bonds. Moreover, the study of the abstraction reaction on an *a*-Si:H surface is complicated by the insertion and etching reactions, which also modify the surface hydrogen coverage. Hence, we used deuterium in place of hydrogen to enable a more detailed understanding of the processes occurring on the surface. Use of deuterium should not drastically alter the conclusions of this study, since the energetics of abstraction of surface H by D and H are expected to be very similar.[11]

The article is structured as follows. In Sec. II, we present in detail the experimental setup, including the plasma reactor and the *in situ* surface diagnostics. In the latter part of this section, we discuss the data collection methodology for the experiments involving *a*-Si:H film deposition and subsequent exposure of these films to a D_2 plasma. In Sec. III, we give our interpretation of the IR and spectroscopic ellipsometry data taking into account the different interactions of D with *a*-Si:H surfaces. We discuss at length the deconvolution of our IR spectra to eliminate the effects of insertion and etching reactions from the abstraction reaction. We summarize our findings in Sec. IV.

II. EXPERIMENT

A. Plasma deposition reactor

The experiments were conducted in a stainless steel, inductively coupled plasma reactor shown schematically in Fig. 2. The plasma is generated by applying radio frequency (rf) power at 13.56 MHz through a matching network to a 15-cm-diameter planar spiral copper coil placed above a quartz window that forms the vacuum seal at the top of the chamber. The chamber is pumped by a 900 l/s turbomolecular pump (Leybold TMP 1000) and the base pressure is $\sim 10^{-5}$ Pa. The distance between the quartz window and the floating substrate platen is approximately 20 cm. The temperature of the substrate is regulated by a feedback controller (Omega 9000A) in conjunction with a 300 W resistive heater

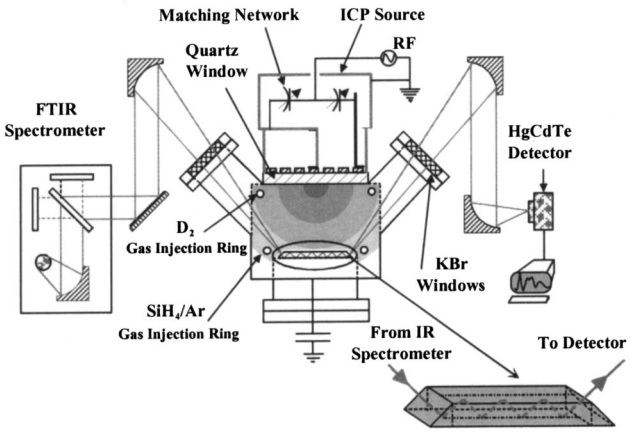

FIG. 2. Schematic of the inductively coupled plasma (ICP) deposition reactor and the *in situ* attenuated total reflection Fourier transform infrared (ATR-FTIR) spectroscopy apparatus. The GaAs internal reflection crystal is shown in detail. The bulk hydrides are probed by the multiple internal transmission through the film and the surface hydrides are probed by the evanescent field that decays exponentially into vacuum. The reactor is also equipped with *in situ* spectroscopic ellipsometry apparatus (SE) which is not shown in the figure.

and a K-type thermocouple placed directly under the sample position. The gases are injected through two separate gas injection rings, located at positions shown in Fig. 2. Silane (1% SiH_4, 99% Ar) is injected close to the substrate and all other gases are injected close to the plasma source. The gas flow rates are regulated by mass flow controllers (BOC Edwards Model 825 Series B). The pressure in the chamber is measured by a capacitance manometer (BOC Edwards Model 655) and maintained independent of the gas flow rate using a gate valve (VAT) regulated by a downstream adaptive pressure controller (VAT PM-5).

B. *In situ* surface characterization

Figure 2 also shows the *in situ* ATR-FTIR apparatus, which was used to monitor the infrared spectra of silicon hydride (deuteride) vibrations in *a*-Si:H films. The experimental setup is similar to the one that has been described in a previous publication.[30] Infrared radiation from a spectrometer (Nicolet 550) is focused by a KBr lens and directed through a KBr window onto one of the beveled edges of the internal reflection crystal as shown in Fig. 2. The IR radiation undergoes multiple total internal reflections through the crystal and emerges from the other beveled edge. After passing though a second KBr window on the opposite reactor wall, the IR radiation is collected by a lens and focused onto a HgCdTe (Nicolet MCT A) detector. Since the refractive indices of GaAs and *a*-Si:H are closely matched, total reflection occurs at the vacuum/film interface and the bulk hydrides and deuterides are probed by the total internal transmission through the film. Surface hydrides and deuterides are probed by the attenuated field, which decays exponentially into vacuum.[31] The IR beam is reflected approximately 40 times on each flat face of the crystal and, hence, passes through the growing film 80 times, greatly enhancing the signal-to-noise ratio. The resolution of the spectrometer was set at 4 cm^{-1} and spectra were collected over the range of

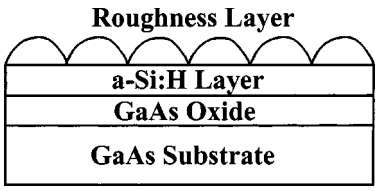

FIG. 3. Three-layer model used to fit the spectroscopic ellipsometry (SE) data.

750–4000 cm^{-1}. Depending on the expected absorption strength, 100 to 500 scans were averaged to improve the signal-to-noise ratio. The sensitivity for our setup in reflectance, R, is $\Delta R/R \approx 10^{-5}$.

The plasma chamber is also equipped with an *in situ* spectroscopic ellipsometer (J. A. Woollam Co., Model M-88) which was used to monitor the changes in film thickness during D_2 plasma exposure. The detailed working principles of spectroscopic ellipsometry (SE) have been discussed elsewhere.[32,33] Briefly, in our experimental setup, broadband light (300–800 nm) from a Xe arc lamp is linearly polarized and directed onto the film surface at an angle of 70° to the surface normal. The change in the reflected beam polarization is measured through a rotating analyzer and an array detector which allows simultaneous detection at 88 wavelengths. Ellipsometry measurements were used to complement IR measurements and to further characterize surface roughening and etching during exposure of the film to D. The SE data were analyzed using a three-layer model on a GaAs substrate as shown in Fig. 3. The first layer is the native oxide on the GaAs crystal, the second one is an *a*-Si:H film which is fitted by the Tauc-Lorentz model,[34,35] and the third one is a surface roughness layer fitted using the effective medium approximation with 50% void fraction in the film.[33]

C. *a*-Si:H film deposition and D_2 plasma exposure

The *a*-Si:H films used in this study were deposited on undoped, double-side polished, trapezoidal GaAs (100) internal reflection crystals. Trapezoidal-shaped, IR-transparent GaAs internal reflection crystals enable multiple total internal reflection infrared spectroscopy for monitoring the change in various silicon hydride and silicon deuteride vibrational modes both in the film and on the surface. The dimensions of the GaAs crystal are 50 mm×10 mm×0.6 mm with the short sides faceted at 45°. Approximately 30 nm thick films were deposited at a substrate temperature of 200 °C in 45 min. The flow rate of the silane-argon mixture was 50 standard cm^3/min (sccm) for all the depositions and the pressure and plasma power were maintained at 26 Pa and 15 W, respectively. The deposited films were deuterated by several one-second pulses of D_2 plasma and the deuterium uptake in the film was observed using ATR-FTIR in between pulses. The deuterium exposure time was controlled accurately and reproducibly by externally triggering the power supply to generate each pulse. Low plasma power (15 W) was used for the deuteration experiment to marginalize the effect of ions. During D_2 plasma exposure, the D_2 flow rate was set at 6 sccm and the chamber pressure was maintained at 26 Pa. The deposited films were cooled to different temperatures (60 °C, 100 °C, 150 °C, 200 °C) in order to study the temperature dependence of the deuteration process. After each deposition and deuteration cycle, the internal reflection crystal and the chamber were cleaned with a CF_4 plasma. The cleaning procedure reconditioned the chamber walls and eliminated the need to vent the chamber by allowing us to use the same internal reflection crystal for different experiments and, hence, improved the reproducibility of the deposition and deuteration processes.

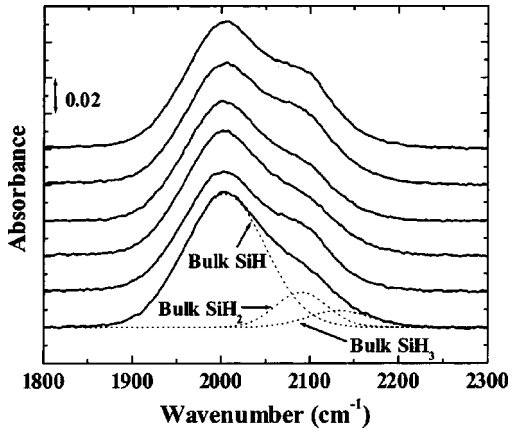

FIG. 4. Infrared spectra obtained during film growth at a substrate temperature of 200 °C. The spectra are offset for clarity and represent only the contribution of bulk hydrides during the last 15 min of film growth. One of the spectra is deconvoluted to show the contributions from different bulk hydrides.

D. Infrared data collection and analysis

All the IR spectra presented in this article were collected in a differential mode where the spectra are recorded with respect to a suitable reference spectrum (background). The

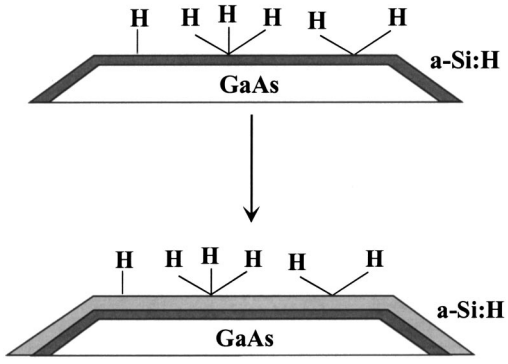

FIG. 5. Illustration of the experiments to determine the bulk silicon-hydride absorptions. The sketch at the top represents the film (dark gray) and the GaAs substrate after 30 min of film growth. The bottom sketch represents the film and the substrate after 15 min of film (light gray) growth on top of the film grown during the first 30 min (dark gray). If the surface hydride concentration and composition remain constant after the first few minutes of growth, their contribution is cancelled by using the film represented in the top figure as background. Hence, the absorbance, $A(\omega)$, due to the last 15 minutes of growth can be expressed as $A_{\text{film}}(\omega) = -\log_{10}(I_{\text{film}})$, where, $I_{\text{film}} = I(\Delta t)/I(t=0)$. $I(t=0)$ and $I(\Delta t)$ are the intensities for the background spectrum ($t=0$) and at $t=\Delta t$, respectively. The absorbance spectra obtained by this method are shown in Fig. 4.

TABLE I. Measured infrared peak positions and their full width at half maximum. The assignments and the distinction between surface and bulk peaks is made on the basis of the absorption frequencies reported in the literature.

	Surface			Bulk		
Species	Position (cm^{-1})	Width (cm^{-1})	References	Position (cm^{-1})	Width (cm^{-1})	References
			Hydrides			
SiH	2069–2084	10–20	37–44	1995–2002	80–105	36,45
SiH_xD_{2-x} $x=1,2$	2106–2112	29–35	37–41	2095	55–70	36
SiH_yD_{3-y}[a] $y=1,2,3$	2130–2140	10–30	38–41,46	2135–2140	40–50	36
SiH_zD_{4-z}[b,c] $z=1,2,3,4$	Not observed	⋯	⋯	2170	60	30,47
			Deuterides			
SiD	Not observed (Expected ~1510)	⋯	⋯	1460–1470	65–70	⋯
SiH_xD_{2-x} $x=0,1$	1523–1527	23–28	38,47–49	1520	50	⋯
SiH_yD_{3-y}[a] $y=0,1,2$	1540–1570	10–20	38,47,48	1550	45	⋯
SiH_zD_{4-z}[c] $z=0,1,2,3$	Not observed	⋯	⋯	1595–1600	30–35	47
Unassigned	⋯	⋯	⋯	1638	25–35	⋯

[a]The bulk frequency assignments for these species are partly based on interpretations in present work. The Si–H and Si–D stretching modes in bulk $Si–H_yD_{3-y}$ $(0\leqslant y\leqslant 3)$ are expected to appear at a frequency very close to the corresponding surface features, since a $Si–H_yD_{3-y}$ $(0\leqslant y\leqslant 3)$ would disrupt the silicon network and trap a void.

[b]The vibrational bands at 2170 cm^{-1} and 2165 cm^{-1} are also attributed to $SiH_2(SiO)$ (Ref. 50) and $SiH(O_2)$, (Ref. 51), respectively, on *c*-Si surface. The *a*-Si:H literature is not very clear on this peak assignment and the vibrational mode appearing at these wavenumbers is often attributed to oxygen contamination in the *a*-Si:H film. We attribute this vibrational band to either physisorbed silane or disilane trapped in the bulk film possibly via an overcoordination defect (see text) (Ref. 30). The temperature dependence of this feature indicates strongly that it cannot be oxygen related.

[c]Can also be the higher silane analogs like disilane.

reference spectrum was chosen to cancel all effects except the effect of the last process the crystal and the film had undergone. For example, during the deuteration experiments, the reference spectrum was taken to be the spectrum of the crystal and the as-deposited *a*-Si:H film at the temperature of D exposure. All spectra taken with respect to this reference during the deuteration process show only the differences in the film due to reactions with D from the D_2 plasma. A decrease in absorption at the characteristic vibration frequency of a particular bond corresponds to removal of these modes. Conversely, an increase in absorption corresponds to creation of modes.

We used the difference between the IR spectra of the film taken at two different times during deposition to obtain the bulk silicon hydride absorptions independent of the surface hydrides. The initial growth on a bare GaAs surface is expected to be different than that on an *a*-Si:H surface. To avoid the effects of the GaAs substrate on the *a*-Si:H film properties, we deposited for 45 min and collected a new background every 15 min. Using ATR-FTIR, we ensured that the surface and bulk film composition and deposition rate reach a steady state after the first 15 min of growth. The second and third interval of 15 min of deposition (which are on an *a*-Si:H surface) produce the same absorbance spectrum; such absorbance spectra are shown in Fig. 4 for six different films that were used in this study. Reproducible spectra, such as those in Fig. 4, are necessary to ensure the reproducibility of the subsequent deuteration process. Since the surface composition is expected to remain the same after reaching steady state, the contribution of the surface silicon hydrides to the IR spectra will be cancelled as shown schematically in Fig. 5. Thus, the spectra shown in Fig. 4 are the IR spectra of the bulk silicon hydrides. These spectra were deconvoluted into three Gaussian peaks centered at ~2000 cm^{-1}, ~2094 cm^{-1}, and ~2140 cm^{-1} corresponding to bulk SiH, SiH_2, and SiH_3, respectively.[36] The 2094 cm^{-1} peak may also include contributions due to SiH on internal surfaces such as voids. Figure 4 also shows a typical deconvoluted spectrum. The films contain primarily mono- and dihydrides with small but detectable amount of tri-hydrides.

The deposited *a*-Si:H films were deuterated at the four different temperatures mentioned above (60 °C, 100 °C, 150 °C, and 200 °C). IR spectra were collected as a function of D exposure with respect to a background spectrum collected immediately before deuteration. D exposure is measured and reported as number of 1-second-long D_2 plasma pulses. The deposited films were stable during the time scale of the experiment, i.e., there was no observable change in the IR spectrum of the film without plasma exposure. Upon exposure to a D_2 plasma, changes are expected to occur both

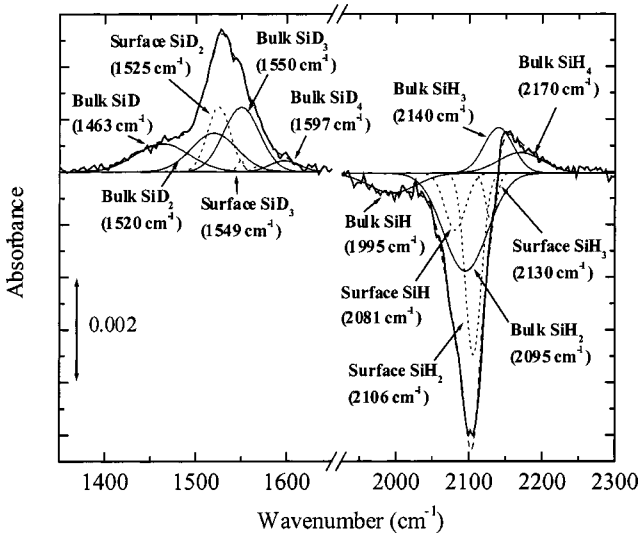

FIG. 6. IR absorbance spectrum obtained after exposure of an *a*-Si:H film to D from a D_2 plasma for 13 s at a substrate temperature of 100 °C. The background was collected before D_2 plasma exposure. The spectrum was deconvoluted using stretching mode frequencies listed in Table I.

on the surface and in the bulk of the film. To distinguish between these changes, the IR absorption bands were deconvoluted in both SiH_x $(1 \leqslant x \leqslant 4)$ and SiD_x $(1 \leqslant x \leqslant 4)$ regions of the spectrum ($x=4$ refers to silane and deuterated silane in internal voids trapped as Si overcoordination defects in the film). Surface and bulk peak assignments for SiH_x and SiD_x features were based on previous IR studies on crystalline, porous, and amorphous silicon and are listed in Table I.[30,36–51] Bulk and surface absorptions can also be distinguished based on their full width at half maximum (FWHM) and their characteristic frequency. Surface absorption bands are much narrower than the corresponding absorptions in the bulk film. On *a*-Si:H films, surface absorptions are typically narrower than 35 cm^{-1}.

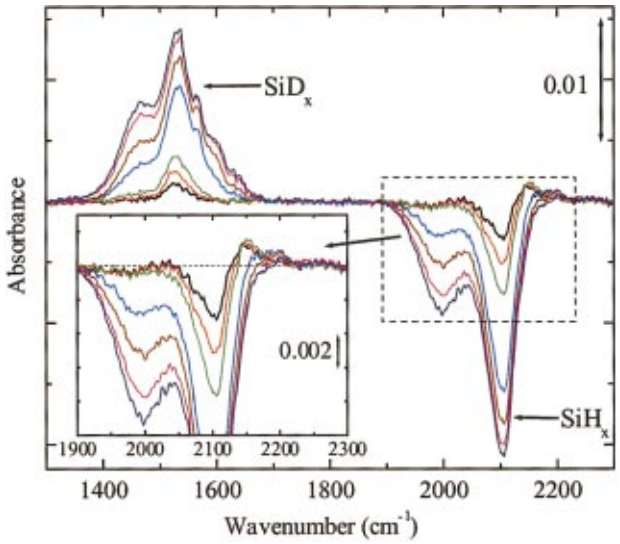

FIG. 7. (Color) Evolution of the IR absorbance spectra obtained during exposure of an *a*-Si:H film to D atoms created in a D_2 plasma at a substrate temperature of 100 °C. The background spectrum was collected before D_2 plasma exposure. The selected spectra shown in the figure represent changes in the film after 3, 5, 8, 38, 78, and 178 s of D_2 plasma exposure, respectively. As D replaces H in the film, an increase in SiD_x $(1 \leqslant x \leqslant 4)$ stretching modes appears at ~1500 cm^{-1} and the corresponding decrease in SiH_x $(1 \leqslant x \leqslant 4)$ stretching modes appears around ~2100 cm^{-1}. The inset shows the initial increase in SiH_3 and physisorbed SiH_4 (as well as their deuterated analogs) at ~2150 cm^{-1} due to insertion of D into strained Si–Si bonds.

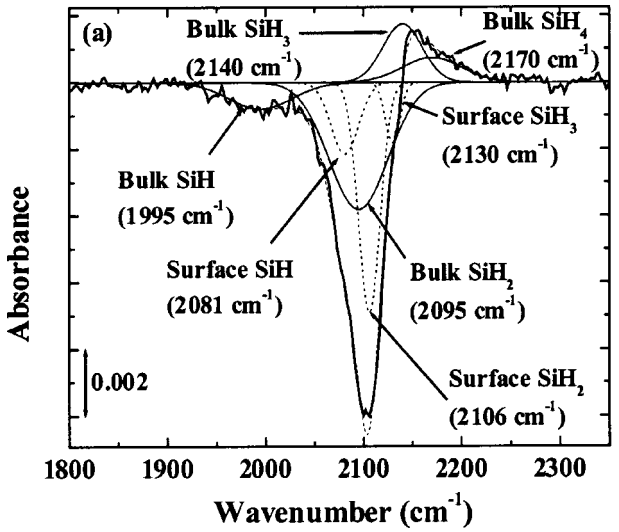

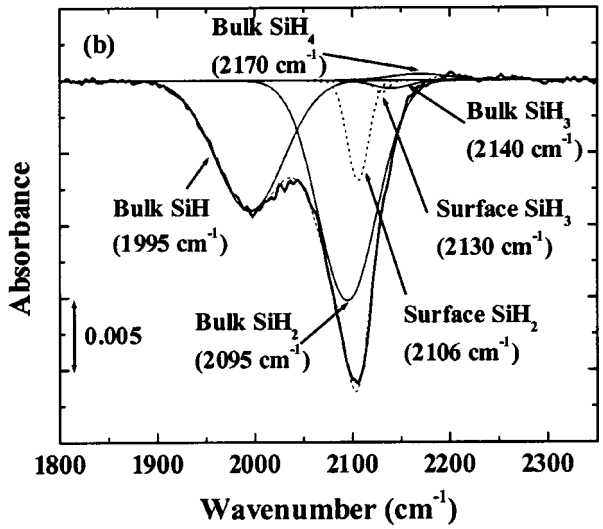

FIG. 8. Changes in the SiH_x $(1 \leqslant x \leqslant 4)$ stretching region of the IR absorbance spectrum for an *a*-Si:H film after exposure to D from a D_2 plasma for (a) 13 s and (b) 178 s at a substrate temperature of 100 °C. The SiH_x $(1 \leqslant x \leqslant 4)$ absorption band was deconvoluted into individual surface and bulk modes as labeled in the figure and listed in Table I.

During D exposure, it is expected that higher hydride and deuteride species present in the film would be mixed, i.e., the same Si atom can be bonded to H as well as D atom(s). However, the observed shifts in peak positions for the hydride stretching modes are not significant if the Si atom is bonded to one or more D atoms.[47] Thus, the dihydride stretching mode in SiHD and SiH_2 and the trihydride stretching mode in $SiHD_2$, SiH_2D, and SiH_3 appear nearly at the same frequency. In the case of higher deuterides, which are formed during D_2 plasma treatment either by exchange or by insertion, the stretching modes can shift depending on the number of H atoms bonded to the Si. This implies that the di-deuteride stretching mode in SiHD and

TABLE II. Reactions of different silicon hydride species with D. The subscripts (s), (g), and (i) denote surface, gas-phase, and interstitial species, respectively. The symbol "_" denotes a dangling bond in a four-fold coordinated Si atom. "Si--Si" indicates a strained silicon-silicon bond. We assume that D immediately passivates all dangling bonds.

	Loss	*Generation*
SiH	Abstraction-passivation[a] (a) $SiH_{(s)} + D_{(g)} \rightarrow Si\_{(s)} + HD_{(g)}$ $Si\_{(s)} + D_{(g)} \rightarrow SiD_{(s)}$ Insertion-passivation (b) $Si\text{--}SiH_{(s)} + D_{(g)} \rightarrow Si\_{(s)} + SiHD_{(s)}$ $Si\_{(s)} + D_{(g)} \rightarrow SiD_{(s)}$	
$Si–H_2$	Abstraction-passivation[a] (c) $SiH_{2(s)} + D_{(g)} \rightarrow SiH\_{(s)} + HD_{(g)}$ $SiH\_{(s)} + D_{(g)} \rightarrow SiHD_{(s)}$ Insertion-passivation (d) $Si\text{--}SiH_{2(s)} + D_{(g)} \rightarrow Si\_{(s)} + SiH_2D_{(s)}$ $Si\_{(s)} + D_{(g)} \rightarrow Si–D_{(s)}$	Insertion-passivation (b) $Si\text{--}Si\text{-}H_{(s)} + D_{(g)} \rightarrow Si\_{(s)} + SiHD_{(s)}$ $Si\_{(s)} + D_{(g)} \rightarrow SiD_{(s)}$
$Si–H_3$	Abstraction-passivation[a] (e) $SiH_{3(s)} + D_{(g)} \rightarrow SiH_{2\_(s)} + H–D_{(g)}$ $SiH_{2\_(s)} + D_{(g)} \rightarrow SiH_2D_{(s)}$ Insertion/etching-passivation (f) $Si\text{--}SiH_{3(s)} + D_{(g)} \rightarrow Si\_{(s)} + SiH_3D_{(i/g)}$ $Si\_{(s)} + D_{(g)} \rightarrow Si–D_{(s)}$	Insertion-passivation (d) $Si\text{--}SiH_{2(s)} + D_{(g)} \rightarrow Si\_{(s)} + SiH_2D_{(s)}$ $Si\_{(s)} + D_{(g)} \rightarrow SiD_{(s)}$
Overall reaction for SiH_x	Total abstraction-passivation (g) $SiH_{x(s)} + D_{(g)} \rightarrow SiH_{(x-1)\_(s)} + HD_{(g)}$ $SiH_{(x-1)\_(s)} + D_{(g)} \rightarrow Si–H_{(x-1)}D_{(s)}$ $x = 1,2,3$ Insertion/etching-passivation (h) $Si\text{--}SiH_{3(s)} + D_{(g)} \rightarrow Si\_{(s)} + SiH_3D_{(i/g)}$ $Si\_{(s)} + D_{(g)} \rightarrow SiD_{(s)}$	

[a]Reactions (a), (c), and (e) have been proposed to occur through a single step in the bulk film (Refs. 23, 24).

SiD_2 and the tri-deuteride stretching mode in $SiDH_2$, SiD_2H, and SiD_3 can appear at different wavenumbers.[47]

The spectra obtained during deuteration were deconvoluted as shown in Fig. 6. Clear changes in absorption due to the silicon hydride and deuteride stretching modes are visible. During deuteration, the silicon-hydride absorptions in the 1950-2250 cm^{-1} region decreased with time as D replaced H in the film and on the surface through abstraction and subsequent passivation. A corresponding increase in silicon deuteride absorptions in the 1400–1700 cm^{-1} region was also detected.

III. RESULTS AND DISCUSSION

A. D(H) insertion into Si–Si bonds

Typical spectra obtained during exposure of an *a*-Si:H film to D at 100 °C through a sequence of 1-s D_2 plasma pulses are shown in Fig. 7. The deconvolution for two of these spectra after 13 and 178 s of D exposure is shown in Figs. 8(a) and 8(b), respectively. Insertion of D into Si–Si bonds is clearly visible in Fig. 8(a) as a prominent absorption feature at 2130–2250 cm^{-1} (also shown in the inset of Fig. 7). This feature in the Si–H stretching region increases during the initial stages of D exposure even though the flux of H atoms to the surface is zero. This increase is detected consistently during the initial stages of low temperature deuteration experiments at 60 °C and 100 °C, but absorption becomes less prominent for longer D exposure as the decreasing bulk SiH_2 peak eventually dominates the spectrum [Fig. 8(b)]. In deconvoluting these spectra, we discovered that they could be best fitted by including absorption peaks centered at ~2140 cm^{-1} and ~2170 cm^{-1}. It is well known that the absorption peak at 2140 cm^{-1} is due to surface SiH_3. However, bulk SiH_3 stretching modes would also appear at the same frequency since SiH_3 would disrupt the connectivity of the amorphous network and create a void region in its vicinity. We assign the absorption at 2170 cm^{-1} to SiH_4 and/or Si_2H_6 trapped in the bulk. Si–H stretching mode in gas-phase silane appears at 2189 cm^{-1} but could shift to lower frequencies when trapped in the bulk film.[52] Disilane in the gas phase absorbs at 2154 cm^{-1} (ν_1) and 2181 cm^{-1} (ν_3).[53] The Si atoms of such species could be overcoordinated in the bulk or on the surface.[30] Regardless of the detailed configuration of these hydrides, the only plausible interpretation for an increase in SiH_3, SiH_4, and/or Si_2H_6 absorptions without H impinging on the surface is that lower hydrides are converted to higher hydrides by insertion of D into Si–Si bonds according to reactions (b), (d), and (f) in Table II. For example, insertion of D into a surface di-hydride would form SiH_2D converting the two Si–H bonds in a di-hydride configuration into two Si–H bonds in a tri-hydride configuration and a Si–D bond in a tri-deuteride configuration. Although

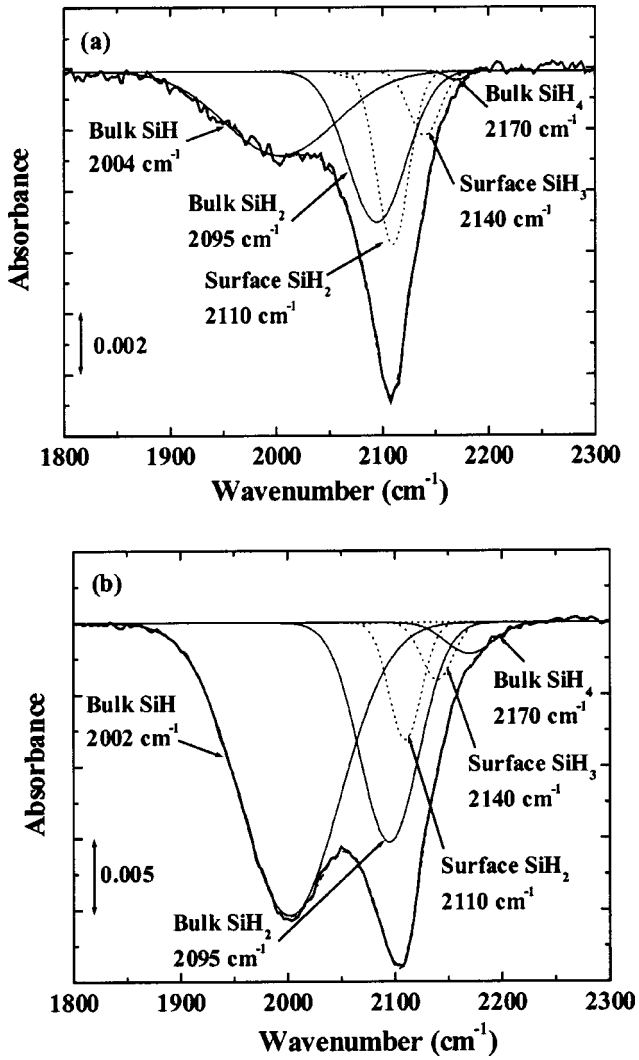

FIG. 9. Changes in the SiH_x ($1 \leqslant x \leqslant 4$) stretching region of the IR absorbance spectrum for an *a*-Si:H film after exposure to D from a D_2 plasma for (a) 13 s and (b) 178 s at a substrate temperature of 200 °C. The SiH_x ($1 \leqslant x \leqslant 4$) absorption band was deconvoluted into individual surface and bulk modes as labeled in the figure and listed in Table I.

the 2140 cm^{-1} and 2170 cm^{-1} features that show a net increase in absorbance are bulk features (Table I), it is obvious that similar processes would occur on the surface as well leading to formation of higher hydrides. However, we do not see a net increase in absorbance due to surface SiH_4 and/or Si_2H_6 because these species are removed by desorption as soon as they are formed. Also, we do not see a net increase in surface SiH_3, because it is removed faster by abstraction than it is formed by insertion into $Si–SiH_2$; this will become evident in Sec. III B.

Absorbance spectra obtained during deuteration at 150 °C and 200 °C do not show an increase at 2140 cm^{-1} and 2170 cm^{-1}. For example, Figs. 9(a) and 9(b) show two deconvoluted spectra obtained after 13 and 178 s of D exposure at 200 °C, respectively. Absence of an absorption increase at these frequencies implies no D insertion into Si–Si bonds or, as it will be shown later, fast decomposition of the higher hydrides at elevated substrate temperatures. This *apparent* lack of insertion at higher temperatures suggests an *apparent* negative activation energy barrier for insertion. Similar results were obtained by Lee *et al.*[54] on a monohydride covered silicon surface which was exposed to D generated using a hot tungsten filament. These authors found that higher hydrides (SiH_2 and SiH_3) were formed due to insertion of H into Si–Si bonds at a substrate temperature of −110 °C. However, insertion was not observed at 200 °C. The authors have suggested three possible reasons for the absence of insertion at 200 °C. First, the products of the insertion reaction do not survive in the film and decompose to mono-hydride by transferring H(D) to a nearby dangling bond which may have been created by abstraction;[55,56] this can explain the observed result even though insertion may be faster at higher temperatures. This H(D) transfer reaction is presumed to be fast and, hence, will not be captured over the time scale of data collection. As a result, in the absorbance spectra, it would appear as if the insertion reaction did not occur. The second possible reason for an *apparent* negative activation energy barrier for insertion is if weakly absorbed D is a precursor for the reaction. The high reactivity of D, however, suggests that a weakly adsorbed precursor-mediated D insertion is unlikely. The third possibility for the loss of tri-hydrides is the formation of disilane on the surface. In that case, one would observe etching, as Si would be removed by desorption of disilane. Nevertheless, our ellipsometry data (Table III) show that the film is not etched at 200 °C for the entire duration of D_2 plasma exposure. In contrast, the film is etched slowly (1 Å/min) at 60 °C. The summary of the ellipsometry data obtained before and after deuteration for 60 °C and 200 °C experiments is shown in

TABLE III. Summary of spectroscopic ellipsometry data.

		60 °C			200 °C		
Substrate temperature	Layer type	GaAs oxide	*a*-Si:H film	Surface roughness layer[a]	GaAs oxide	*a*-Si:H film	Surface roughness layer[a]
Layer thickness (Å)	Before deuteration	20	332	76	19	344	62
	After deuteration	20	329	76	19	344	62

[a]The SE measurements were performed over an area of 1–2 mm^2 and, hence, capture the global roughness on the film surface. Surface roughness was measured using atomic force microscopy, for films grown in our reactor under similar conditions and the root mean square roughness was less than 20 Å.

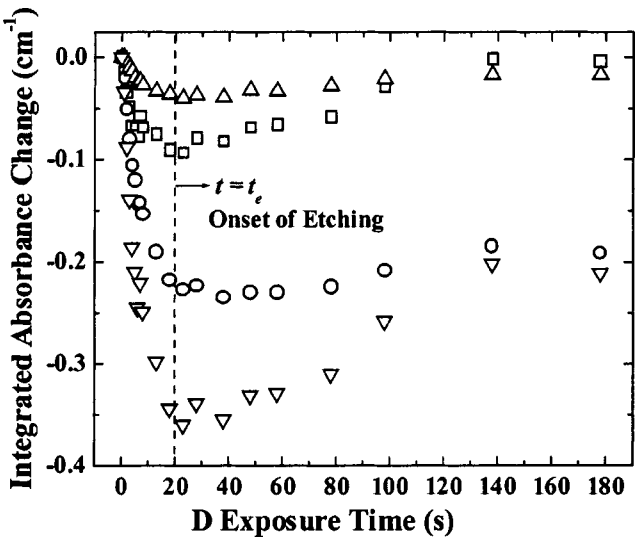

FIG. 10. Temporal evolution of surface SiH (□), SiH_2 (○), SiH_3 (△) and total SiH_x (▽) absorbance during D_2 plasma exposure at a substrate temperature of 100 °C. The data collection intervals were chosen to capture the rapid initial changes in the film composition. The vertical dashed line indicates the onset of etching.

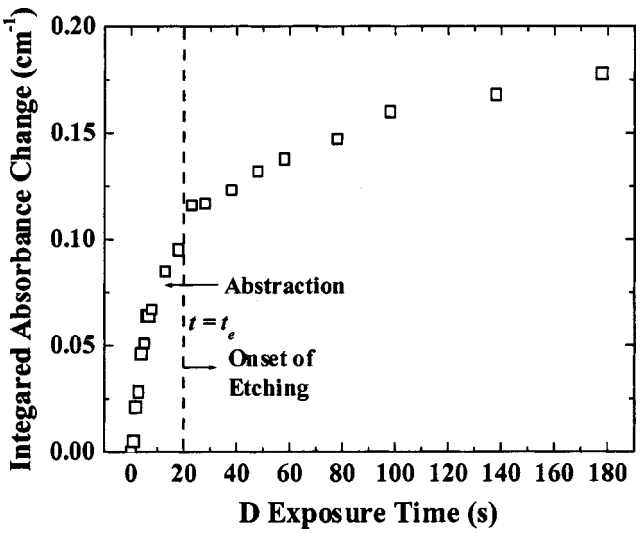

FIG. 12. Temporal evolution of the surface silicon deuteride absorptions during D_2 plasma exposure at a substrate temperature of 100 °C. During the initial stages of exposure ($t<t_e$), SiD_x absorption increases rapidly and linearly followed by a much slower increase during the latter stages of D exposure ($t>t_e$). The point at which the slope changes ($t=t_e$) corresponds to the minimum in Fig. 11 and indicates the onset of etching.

Table III. Based on our ellipsometry results, the first mechanism seems to be the most plausible explanation for the *apparent* negative activation energy barrier for insertion. Thus, we conclude that insertion occurs at all temperatures but the insertion products rapidly decompose at high temperatures.

B. Decoupling abstraction, insertion, and etching

The spectra collected during deuteration, such as those shown in Fig. 7, were deconvoluted as described in Sec. II D and the temporal evolution of the integrated absorbance due to different stretching modes was determined at each of the four different substrate temperatures. Figure 10 shows the integrated absorbance for surface mono-, di-, and trihydrides (area under the corresponding Gaussian peak), and total surface hydrides as a function of D exposure time for a deuteration experiment conducted at 100 °C. All of the reactions shown in Table II occur at the same time and influence the temporal evolution of the surface silicon hydride coverage, which makes the extraction of kinetic information from Fig. 10 difficult. For example, SiH_3 modes are removed by the abstraction-passivation reaction and insertion into $Si–SiH_3$. They are created by insertion of D into $Si–SiH_2$ bonds. Similar reactions also occur for SiH and SiH_2. All of the reactions that generate and deplete various silicon hydrides are listed in Table II. At each substrate temperature, the effects of the insertion and abstraction reactions have to be decoupled to obtain the rate constant for abstraction.

A simple way of decoupling the insertion and abstraction reactions would be to add up all the reactions shown in Table

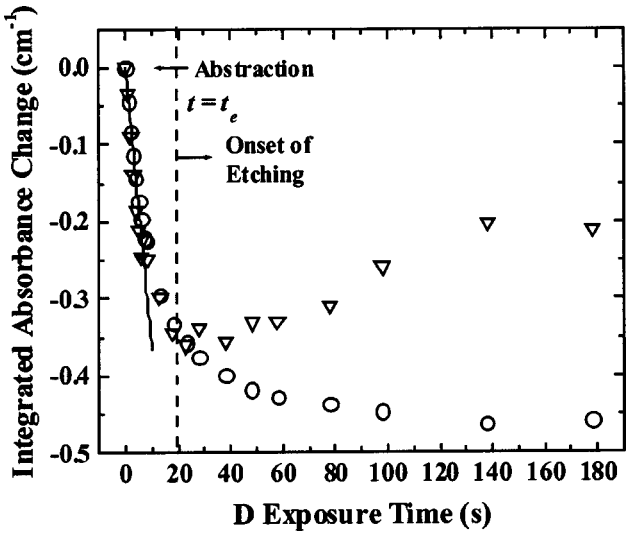

FIG. 11. Temporal evolution of the total surface silicon-hydride absorptions on *a*-Si:H films as a function of D_2 plasma exposure time at substrate temperatures of 100 °C (▽) and 200 °C (○). The data for 100 °C show a minimum in the SiH_x absorptions indicating the onset of etching ($t=t_e$), whereas the data for 200 °C show an exponential decrease in SiH_x absorption. The initial part of the curve in both cases is linear with the same slope, which is proportional to the abstraction rate.

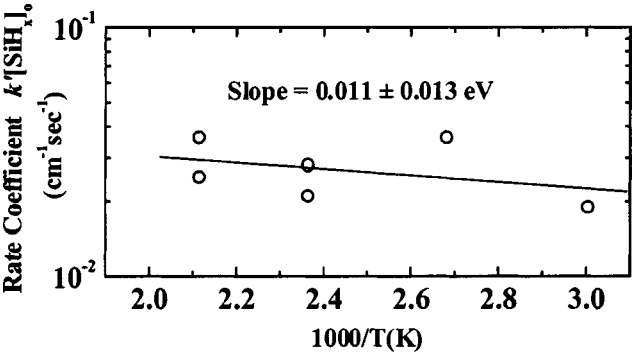

FIG. 13. Arrhenius plot for the temperature dependence of the abstraction reaction rate coefficient. The small value of the slope and the comparable value of error in the fit indicate that within the accuracy of the experiments there is practically no activation energy barrier for abstraction of H by D from an *a*-Si:H surface.

II for the loss and generation of all the hydrides. This summation cancels out the effect of insertion into the mono- and di-hydride species and results in two overall reactions (g) and (h). The overall abstraction reaction (g) shown in Table II results from summing up all the abstraction-passivation reactions while reaction (h) is the etching reaction. Etching by insertion into $Si–SiH_3$ has to be decoupled from the abstraction reactions. We decouple abstraction from etching by using a primarily di-hydride covered surface. In our reactor, the *a*-Si:H films deposited at 200 °C are covered primarily with silicon di-hydride.[31,57,58] Hence, during the initial stages of D exposure we would mainly expect conversion of the di-hydrides to partially deuterated tri-hydrides by D insertion into $Si–SiH_2$; this provides a short time window during which abstraction can be observed without etching. Therefore, separation of abstraction from insertion into mono- and di-hydrides can be resolved if we can identify the onset of etching (insertion into $Si–SiH_3$) in Fig. 10.

The procedure for decoupling abstraction and etching to obtain the abstraction rate has two inherent assumptions: the different surface hydrides are abstracted with the same probability and the IR absorption cross sections are the same for the different hydride species. On the first assumption, Koleske *et al.*[11] measured a reduced abstraction rate of H from a Si(100) surface by D when the surface hydride coverage was increased. These authors estimated 25% of higher hydrides on the surface (24% di-hydride and 1% tri-hydride). However, it is not clear if the reduced abstraction rate is due to surface roughening or difference in the abstraction cross section for the different hydrides. In contrast, Flowers *et al.*[59] observed the same abstraction rate from mono- and di-hydrides on a *c*-Si surface. Regarding the second assumption, there is indirect evidence that it may be fairly accurate.[31,57,58] Regardless of the above assumptions, the results obtained with this procedure should be accurate at least for abstraction of H from silicon di-hydride; this is because our initial surface is di-hydride dominated.

The onset of etching can be identified from the temporal evolution of the IR absorption data. Figure 11 shows that initially the decrease in total hydride concentration is almost linear. However, at lower deuteration temperatures (60 °C and 100 °C) and longer D exposure times, the curve reaches a minimum and then begins to rise again. Careful analysis of the data in Fig. 10 and spectroscopic ellipsometry data show that the minimum in the curve indicates the onset of etching. First evidence for *a*-Si:H etching is the apparent increase in the SiH_x absorption on the surface for $t>t_e$. In the absence of a hydrogen source from the plasma, the increase in absorption for the silicon hydride stretching modes can only result due to the onset of etching, which can have two effects on the film surface. First, an increase in absorbance can result from the removal of surface atoms exposing hydrides from the subsurface whose hydrogen atoms have not yet been abstracted. Second, the absorbance due to surface features can increase due to an apparent increase in the surface area of the film due to roughening which can also be caused by etching. The subsurface is expected to contain mono- and di-hydrides at concentrations much higher than that of tri-hydrides. Figure 10 indeed shows that only the lower hydrides increase for $t>t_e$. Both ellipsometry and the temporal evolution of the surface silicon deuteride features during deuteration further support this hypothesis. The ellipsometry data collected before and after deuteration at 60 °C substrate temperature indicates that the film thickness decreases by ~3 Å in 3 min, whereas, at 200 °C we do not observe any etching. The temporal evolution of surface deuterides at 100 °C has two distinct slopes as shown in Fig. 12. Initially, there is a rapid increase in absorption followed by a slow rise for longer D exposure times. The point at which the slope changes ($t=t_e$) corresponds to the extremum observed in the evolution of the surface hydride coverage. This slow increase in the surface deuterides is due to the same reason as the increase in surface hydrides. Hence, the abstraction reaction rate at different temperatures can be obtained only from the initial linear decrease for $t<t_e$.

C. Activation energy barrier of the abstraction reaction

If abstraction proceeds via an Eley–Rideal mechanism, it is described completely by

$$SiH_{x(s)} + D_{(g)} \xrightarrow{k} SiH_{x-1(s)} + HD_{(g)}. \tag{1}$$

The rate expression for the reaction in Eq. (1) can be written as

$$\frac{d[SiH_x]}{dt} = -k \cdot F_D \cdot [SiH_x], \tag{2}$$

where $[SiH_x]$ represents the density of Si–H bonds on the surface in cm^{-2}, F_D is the flux of D atoms to the surface in $cm^{-2}\,s^{-1}$, k is the temperature dependent rate constant for the reaction in cm^2, and t is the time for the reaction in seconds. The reaction is pseudo-first order if the flux of deuterium to the surface is kept constant. Integration of Eq. (2) yields

$$\frac{[SiH_x]_t}{[SiH_x]_o} = \exp(-k' \cdot t), \tag{3}$$

where $k' = F_D \cdot k$, and $[SiH_x]_t$ and $[SiH_x]_o$ are the surface concentration of the silicon hydrides at time t and $t=0$, respectively. In IR spectroscopy, only the changes in the surface hydride concentration are detected and it is convenient to express Eq. (3) as

$$\begin{aligned}\Delta[SiH_x] &= [SiH_x]_t - [SiH_x]_o \\ &= -[SiH_x]_o \cdot (1 - \exp(-k' \cdot t)),\end{aligned} \tag{4}$$

where the change in IR absorption is proportional to the change in $SiH_x (1 \leqslant x \leqslant 3)$ concentration on the surface. The abstraction reaction can be observed without interference from etching only for small t, consequently, Eq. (4) can be linearized in the small t limit yielding

$$\Delta[SiH_x] = [SiH_x]_t - [SiH_x]_o = -[SiH_x]_o \cdot k' \cdot t. \tag{5}$$

Figure 11 shows the temporal evolution of $[SiH_x]_t - [SiH_x]_o$ for experiments conducted at 100 °C and 200 °C. The slope of these plots for small t is $[SiH_x]_o \cdot k'$. Hence, we calculate the abstraction rate by fitting a straight line through the initial part of the data. It is important to note that the slope is

also dependent on the initial hydride coverage of the film and it is essential that the films be deposited at the same temperature before the deuteration process to ensure the same initial hydride coverage for each experiment. The temperature dependence of the rate constant k is expressed by the usual Arrhenius form, $k=k_o\cdot\exp(-E_a/k_B\cdot T)$, where k_o is the preexponential factor, E_a is the activation barrier for the reaction, k_B is Boltzmann's constant and T is absolute temperature. The abstraction rates determined from the initial slopes in Fig. 11 were plotted as a function of temperature in the Arrhenius plot shown in Fig. 13. The slope of the straight line fit through the data plotted in Fig. 13 gives an activation barrier of 0.011 ± 0.013 eV. Within the accuracy of the experimental data, we conclude that the slope of the line is practically zero. This indicates that the abstraction rate is independent of temperature. This result is in agreement with our atomistic simulations for the abstraction of atomic hydrogen from a-Si:H surfaces by H from the gas phase.[60–62]

IV. CONCLUSIONS

In summary, we determined the activation energy barrier for the abstraction of H by D from an a-Si:H surface by carefully deconvoluting from IR spectra the effects of the abstraction reaction from insertion and etching reactions. The abstraction rate was found to be independent of temperature, suggesting that there is no activation energy barrier for the abstraction reaction. The insertion of D into strained Si–Si bonds on the amorphous surface was found to occur at a rate comparable to that for abstraction, in the sense that both abstraction and insertion are observed in experiments conducted over times ranging from a few seconds to hundreds of seconds. The similarity of our result to abstraction of H from c-Si surfaces and Si surfaces prepared by other means suggests that abstraction of H is practically independent of the structure of the Si surface and occurs through an Eley–Rideal mechanism.

ACKNOWLEDGMENTS

This work was supported by the NSF/DoE Partnership for Basic Plasma Science and Engineering (Award No. ECS-0078711) and by the Camille & Henry Dreyfus Foundation through Camille Dreyfus Teacher-Scholar awards to two of the authors (E.S.A. and D.M.). A.T. acknowledges support by Fuji Electric Co., Ltd. The authors acknowledge Dr. H. Fujiwara (National Institute of Advanced Industrial Science and Technology, Japan) for suggestions with spectroscopic ellipsometry data analysis and Dr. W. M. M. Kessels (Eindhoven University of Technology, The Netherlands) for many insightful discussions.

[1] A. Matsuda, Thin Solid Films **337**, 1 (1999).
[2] J. R. Abelson, Appl. Phys. A **56**, 493 (1993).
[3] A. Shah, P. Torres, R. Tscharner, N. Wyrsch, and H. Keppner, Science **285**, 692 (1999).
[4] R. A. Street, *Hydrogenated Amorphous Silicon* (Cambridge University Press, Cambridge, 1992).
[5] D. L. Staebler and C. R. Wronski, Appl. Phys. Lett. **31**, 292 (1977).
[6] W. M. M. Kessels, A. H. M. Smets, D. C. Marra, E. S. Aydil, D. C. Schram, and M. C. M. van de Sanden, Thin Solid Films **383**, 154 (2001).
[7] S. Sriraman, S. Agarwal, E. S. Aydil, and D. Maroudas, Nature **418**, 62 (2002).
[8] J. R. Abelson, L. Mandrell, and J. R. Doyle, J. Appl. Phys. **76**, 1856 (1994).
[9] J. R. Abelson, J. R. Doyle, L. Mandrell, A. M. Myers, and N. Maley, J. Vac. Sci. Technol. A **8**, 1364 (1990).
[10] W. H. Weinberg, in *Advances in Gas-Phase Photochemistry and Kinetics*, edited by M. N. R. Ashfold and C. T. Rettner (The Royal Society of Chemistry, Letchworth, 1991), p. 171.
[11] D. D. Koleske, S. M. Gates, and B. Jackson, J. Chem. Phys. **101**, 3301 (1994).
[12] K. Sinniah, M. G. Sherman, L. B. Lewis, W. H. Weinberg, J. T. Yates, Jr., and K. C. Janda, J. Chem. Phys. **92**, 5700 (1990).
[13] D. D. Koleske, S. M. Gates, and J. A. Schultz, J. Chem. Phys. **99**, 5619 (1993).
[14] W. Widdra, S. I. Yi, R. Maboudian, G. A. D. Briggs, and W. H. Weinberg, Phys. Rev. Lett. **74**, 2074 (1995).
[15] S. A. Buntin, J. Chem. Phys. **108**, 1601 (1998).
[16] W. H. Weinberg, Acc. Chem. Res. **29**, 479 (1996).
[17] A. Dinger, C. Lutterloh, and J. Kuppers, Chem. Phys. Lett. **311**, 202 (1999).
[18] E. Srinivasan, H. Yang, and G. N. Parsons, J. Chem. Phys. **105**, 5467 (1996).
[19] K. Nakajima, K. Miyazaki, H. Koinuma, and K. Sato, J. Appl. Phys. **84**, 606 (1998).
[20] K. G. Nakamura, Chem. Phys. Lett. **285**, 21 (1998).
[21] C.-M. Chiang, S. M. Gates, S. S. Lee, M. Kong, and S. F. Bent, J. Phys. Chem. B **101**, 9537 (1997).
[22] A. von Keudell and J. R. Abelson, J. Appl. Phys. **84**, 489 (1998).
[23] B. Tuttle, C. G. Van De Walle, and J. B. Adams, Phys. Rev. B **59**, 5493 (1999).
[24] M. Kemp and H. M. Branz, Phys. Rev. B **52**, 13946 (1995).
[25] Y. Muramatsu and N. Yabumoto, Appl. Phys. Lett. **49**, 1230 (1986).
[26] E. Srinivasan and G. N. Parsons, Appl. Phys. Lett. **72**, 456 (1998).
[27] E. S. Aydil and R. A. Gottscho, Solid State Technol. **40**, 181 (1997).
[28] Y. J. Chabal, Surf. Sci. Rep. **8**, 211 (1988).
[29] D. C. Marra, E. A. Edelberg, R. L. Naone, and E. S. Aydil, Appl. Surf. Sci. **133**, 148 (1998).
[30] D. C. Marra, E. A. Edelberg, R. L. Naone, and E. S. Aydil, J. Vac. Sci. Technol. A **16**, 3199 (1998).
[31] D. C. Marra, Ph.D. Dissertation, University of California, Santa Barbara (2000).
[32] D. E. Aspnes, J. Vac. Sci. Technol. **18**, 289 (1981).
[33] D. E. Aspnes, Thin Solid Films **89**, 249 (1982).
[34] G. E. Jellison and F. A. Modine, Appl. Phys. Lett. **69**, 2137 (1996).
[35] G. E. Jellison and F. A. Modine, Appl. Phys. Lett. **69**, 371 (1996).
[36] G. Lucovsky, R. J. Nemanich, and J. C. Knights, Phys. Rev. B **19**, 2064 (1979).
[37] Y. J. Chabal and K. Raghavachari, Phys. Rev. Lett. **53**, 282 (1984).
[38] V. A. Burrows, Y. J. Chabal, G. S. Higashi, K. Raghavachari, and S. B. Christman, Appl. Phys. Lett. **53**, 998 (1988).
[39] Y. J. Chabal, G. S. Higashi, K. Raghavachari, and V. A. Burrows, J. Vac. Sci. Technol. A **7**, 2104 (1989).
[40] U. Jansson and K. J. Uram, J. Chem. Phys. **91**, 7978 (1989).
[41] K. J. Uram and U. Jansson, J. Vac. Sci. Technol. B **7**, 1176 (1989).
[42] Y. J. Chabal, G. S. Higashi, and S. B. Christman, Phys. Rev. B **28**, 4472 (1983).
[43] P. Jakob, P. Dumas, and Y. J. Chabal, Appl. Phys. Lett. **59**, 2968 (1991).
[44] P. Jakob, Y. J. Chabal, and K. Raghavachari, Chem. Phys. Lett. **187**, 325 (1991).
[45] M. H. Brodsky, M. Cardona, and J. J. Cuomo, Phys. Rev. B **16**, 3556 (1977).
[46] K. J. Uram and U. Jansson, Surf. Sci. **249**, 105 (1991).
[47] J. A. Glass, Jr., E. A. Wovchko, and J. T. Yates, Jr., Surf. Sci. **348**, 325 (1996).
[48] Y. Toyoshima, A. Matsuda, and K. Arai, J. Non-Cryst. Solids **166**, 103 (1993).
[49] Y. J. Chabal and K. Raghavachari, Phys. Rev. Lett. **54**, 1055 (1985).
[50] M. Niwano, Surf. Sci. **428**, 199 (1999).
[51] M. K. Weldon, B. B. Stefanov, K. Raghavachari, and Y. J. Chabal, Phys. Rev. Lett. **79**, 2851 (1997).
[52] H. W. Kattenberg and A. Oskam, J. Mol. Spectrosc. **49**, 52 (1974).
[53] H. S. Gutowsky and E. O. Stejskal, J. Chem. Phys. **22**, 939 (1954).

[54] S. S. Lee, M. J. Kong, S. F. Bent, C.-M. Chiang, and S. M. Gates, J. Phys. Chem. **100**, 20015 (1996).
[55] S. Ramalingam, D. Maroudas, and E. S. Aydil, J. Appl. Phys. **86**, 2872 (1999).
[56] S. P. Walch, S. Ramalingam, E. S. Aydil, and D. Maroudas, Chem. Phys. Lett. **329**, 304 (2000).
[57] D. C. Marra, W. M. M. Kessels, M. C. M. van de Sanden, K. Kashefizadeh, and E. S. Aydil, J. Vac. Sci. Technol. A (submitted).
[58] W. M. M. Kessels, Ph.D. Dissertation, Eindhoven University of Technology (2000).
[59] M. C. Flowers, N. B. H. Jonathan, A. Morris, and S. Wright, Surf. Sci. **396**, 227 (1998).
[60] S. Ramalingam, Ph.D. Dissertation, University of California, Santa Barbara (2000).
[61] D. Maroudas, Adv. Chem. Eng. **28**, 251 (2001).
[62] S. Agarwal, S. Sriraman, A. Takano, M. C. M. van de Sanden, E. S. Aydil, and D. Maroudas, Surf. Sci. **515**, L469 (2002).